BJRS

BRAZILIAN JOURNAL
OF
RADIATION SCIENCES
07-02A (2019) 01-13

Study on welding thermal cycle and residual stress of UNS S32304 duplex stainless steel selected as external shield for a transport packaging of Mo-99

Betini[a] E.G., Gomes[a] M.P., Milagre[a] M.X., Machado[a] C.S.C., Reis[a] L.A.M., Mucsi[a] C.S., Orlando[b] M.T.D., Luz[b] T.S., Martinez[a] L. G., Rossi[a] J.L.

[a] *Universidade de São Paulo - USP, Instituto de Pesquisas Energéticas e Nucleares - IPEN/CNEN, 05508-000, São Paulo/ SP, Brazil*

[b] *Universidade Federal do Espirito Santo - UFES, Dep. de Engenharia Mecânica – DEM, 29075-910, Vitória/ES, Brazil*

egbetini@ipen.br

ABSTRACT

Thin plates of duplex stainless steel UNS S32304 were welded using the pulsed gas tungsten arc GTAW process (butt joint) without filler addition. The used shielding gas was pure argon and 98% argon plus 2% of nitrogen. The thermal cycles were acquired during welding, in regions near the melting pool. This alloy is candidate for the external clad of a cask for the transport of high activity radiopharmaceuticals substances. For the residual stress measurements in austenite phase an X-ray diffractometer was used in a Bragg-Brentano geometry with CuKα radiation (λ= 0.154 nm) and for ferrite phase was used a pseudo-parallel geometry with CrKα radiation (λ= 0.2291nm). The results of residual stress using $\sin^2\psi$ methodology showed that the influence of the high welding temperature leads to compressive stresses for both phases of the duplex steels mainly in the heat-affected zone. It was observed a high temperature peak and an increase of the mean residual stress after addition of nitrogen to the argon shielding gas.

Keywords: thermal cycle, residual stress, duplex stainless steel, welding, Mo-99, radioactive material.

ISSN: 2319-0612
Accept Submission 2019-01-14

1. INTRODUCTION

The packaging or cask for the transport of substances that exhibits high gamma ray radioactivity requires adequate thermo-mechanical protection; mainly if tungsten alloys or depleted uranium shielded devices are used for the transport of the Mo-99 with activity above 0.6 TBq (16.2Ci) [1,2]. The increased reliability of the welding process on duplex stainless steels (DSS) for applications in the nuclear industry endorse of the choice this material as external shield for Type B packages [3,4]. The CNEN and IAEA safety standards [5,6] define key parameters for the design, project and validation tests of the transport devices for radioactive materials. The main rules established for external recipient of Type B packages are the thermal and mechanical tests. The first one consists in fully enclose the sample cask in a fire presenting average flame temperature of 800 °C for 30 minutes without loss or dispersal of the radioactive content. For the mechanical properties of the external cask material it is required an ultimate strength of 345 MPa and 189 GPa, for the Young's modulus (as minimum values accepted). For the thermal and impact protection, it is interesting that the material used for the external cask layer presents a low density of around 8100 $kg.m^{-3}$. In order to deal with this, in a study about the selection of materials for a new Type B package, Hara *et al*. defines that the material selected for cask´s external layer belongs to the family of stainless steels and nickel (Ni) alloys. However, the stainless steels present a significantly reduced and competitive price when compared to Ni alloys, showing advantage in their choice [1].

The modern DSS have basically ferritic-austenitic microstructure (around 50 – 50 % ratio) that exhibits excellent properties combining high corrosion resistance and superior mechanical properties. Allied to a competitive cost, the duplex stainless steel grades also have satisfactory weldability [3].

Despite the great advantages there are also some limitations generated during the exposure of the DSS to the high welding temperatures. During the welding cycle, thermal strains are induced in all regions adjacent to the welding [7]. The thermal strains caused during rapid heating are accompanied by plastic upsetting. The thermal stresses resulting from these strains combine and react to produce internal forces that cause residual stress [8]. In previous work, Machado *et al*. [9] studied the effect of the shielding gas composition on the residual stress distribution in the austenite phase of the duplex stainless steel welds. Concerning the radiation influences, Cárcel-Carrasco *et al*. [10]

investigated the effect of low-level ionizing X-rays on the microstructural characteristics, resistance, and corrosion resistance of welded joints of AISI 304 steels by using gas tungsten arc welding (GTAW) process with AISI 316L as filler rods. It was observed that welds subjected to doses of 1000 Gy of ionizing radiation have an influence on its mechanical resistance and corrosion characteristics, and this is especially true for welds made in natural atmospheric conditions. In this way, the concern about these types of failures enhance when dealing with the transportation of radioactive products.

For each type of stress state, it is associated one or a combination of methods for the determination of the residual stresses, to get the best response from the experiments. The most usual methods are: X-ray and neutron diffraction; extensometric blind hole, cut ring, cut by section and removing layers. The X-ray diffraction is considered the most adequate nondestructive method for superficial residual stress measurements. Applied stresses, as external loads, are usually higher at the surface where the failures start over [11, 12, 13].

In this paper it is proposed the analysis of the thermal cycle of welding and residual stress of DSS welded plates for application in the external layer of a new container or cask, for radiopharmaceuticals transport. Temperature curves were acquired during experimentally controlled gas tungsten arc welding (GTAW) process in different positions from the joint line in order to optimize parameters and the soundness better quality of the fabricated parts.

2. MATERIALS AND METHODS

DSS sheet specimens were produced with dimensions 72 x 72 x 1.8 mm^3 and subsequently butt-welded autogenously by the GTAW process in the Welding Laboratory of the Federal University of Espírito Santo (LabSolda/DEM/UFES). Table 1 shows the chemical composition of the UNS S32304 duplex stainless steel used in the experimental work. The alloy's chemical composition was certified by the commercial supplier Aperam Inox América do Sul S/A.

For welding process, pulsed current and direct polarities were used with automatic drive systems. The samples were fixed in order to reproduce the conventional welding process, as shown in Fig. 1. A batch of samples was welded with commercial purity argon as shielding gas and another batch

was welded using a mixture of argon plus 2% of nitrogen. The gas flows rate on the welds in both cases were 10 L.min^{-1}.

Table 1: Chemical composition (% mass and ppm) of the duplex stainless steel UNS S32304

Cr	Ni	Mo	Mn	Si	C	P	S	Ti	Cu	Co	N ppm
22.2	3.5	0.2	1.4	0.25	0.02	0.02	0.001	0.004	0.41	0.091	1030

Figure 1: *Welding arrangement for the duplex stainless steel UNS S32304 thin plates.*

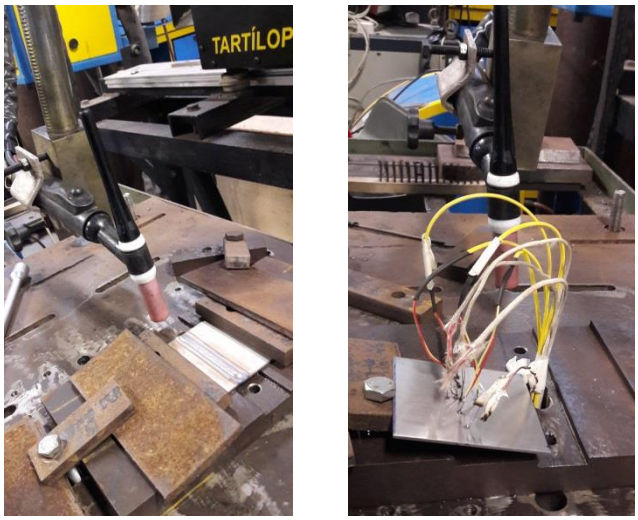

The AWS Class EWTh-2 electrode was kept negative being located at 2 mm at a 90° angle to the plates, according to direct polarity welding GTAW process. For the pulsed current, the square wave was kept balancing background and pulse currents with equal times of 0.9 s. In Table 2, it's shown the welding and thermal cycle parameter.

Regarding the parameters such as voltage (U), pulsed and background currents (Ip, Ib), pulsed and background times (tp, tb), the welding speed (v) along with 0.6 arc efficiency for the pulsed GTA welding, it was possible to calculate the welding heat input (H) per mm using Eq. 1 [8]. The welding heat input shown in Table 2 was determined using the average voltage, current and the average weld speed.

$$H = \frac{60.U.(Ip.tp+Ib.tb)}{(tp+tb).v} \quad (1)$$

The temperature was measured and recorded using K-type thermocouples attached to a data acquisition system. Four thermocouples were positioned and fixed to the sample plate's surface (Fig.2), using high voltage capacitive discharge generator at different distances, along transversal and longitudinal lines of the weld bead. The thermocouples were located at 3.0 mm, 3.5 mm, 4.0 mm and 5.0 mm from the joint line.

Table 2: Welding parameters used for the pulsed GTAW process.

Sample	#WA	#WAN
Shielding gas *(10L.min^{-1})*	Pure Argon	Ar+2%N_2
Voltage	11 V	11 V
Pulse current (I_p)	150 A	140 A
Background current (I_b)	80 A	70 A
Pulse time (t_p)	0.9 s	0.9 s
Background time (t_b)	0.9 s	0.9 s
Welding speed	35 cm.min^{-1}	35 cm.min^{-1}
Arc efficiency	60%	60%
Heat Input	0.20 kJmm^{-1}	0.17 kJmm^{-1}

The signals from the thermocouples were acquired in a multi-channel universal data acquisition system (DAQ) amplifier using MX boards - PT1000, at each channel, for room temperature automatic conditioning. The measured total error limit at 300 K room temperature is ± 1 K and the temperature drift (K-type) was used K/10K ratio where the uncertainty was ≤ ± 0.5.

For the residual stress measurement, the X-ray diffraction method was used performing the multiple exposure technique, according to SAE HS-784 standard [14]. This method allows obtaining a more precise determination of ψ (Psi) that represent the angle between specimen surface normal (Ns) and the normal diffracting planes. Strain ε values are recorded for different sample tilt angle (ψ) at constant azimuth angle ϕ. Strain ε vs $\sin^2\psi$ is plotted to estimate the stress values. Measurements were performed in transverse axis of the plate crossing the weld bead. The location of the residual stress measurements were solidified zone (SZ), heat-affected zone (HAZ) and base metal (BM) for both samples. The distances for each measurement are shown in Table 3.

Table 3: All positions for residual stress measurement.

Phase	Distance from the joint line (mm)									
	SZ	**HAZ**				**BM**				
Austenite	0.0	3.5	5.5	8.5	10	-	14	-	-	24
Ferrite	-	3.5	5.5	7.5	9.5	11.5	13.5	15.5	17.5	19.5

For the residual stress measurements in the austenite phase, plane (420), a Rigaku X-ray diffractometer was used in a Bragg-Brentano geometry and CuKα radiation (λ= 0.154 nm). And then, to investigate the residual stress in the ferrite phase, plane (211), a Rigaku X-ray diffractometer was used in a pseudo-parallel geometry and CrKα radiation (λ= 0.229 nm).

The sample was set at position ϕ= 0 ° and, in some cases, ϕ = 90 ° in the direction of rolling. The residual stresses were calculated by the $\sin^2\psi$ method. For the determination of position 2θ of the analyzed plane, the localization method was used according to intensity using the mathematical function Pearson7A [15] and the graphical program FityK [16]. The choice of the function was based on the literature and on the correlations obtained when comparing the results with other functions. For this analysis, the elastic constants are shown in Table 4.

Table 4: Elastic constants of the phases analyzed in the rolling direction (RD) and transversal direction (TD) [17].

Phase	Poisson Coefficient (ν)	Modulus of elasticity (E)
Austenite RD	0.305	190 GPa
Austenite TD	0.281	186 GPa
Ferrite RD	0.186	201 GPa
Ferrite TD	0.333	226 GPa

3. RESULTS AND DISCUSSION

3.1 Thermal Cycle

Fig. 2 shows the welded plates after the pulsed GTAW process along with the positions of the thermocouples. It was observed that the welding line width for the pure Ar as shielding gas flux is less (around 10 mm, see Fig. 2 (a)) than the welded plate with Ar+2%N_2 shielding gas flux (12 mm,

in Fig. 2 (b)). In addition, the welding process using Ar+2%N_2 also presented a visible thermal damage in welding zone.

The temperature distributions for the four thermocouples were plotted for both specimens in Fig. 3. First, Fig. 3 (a) the thermocouples TK1 and TK2 (3.0 mm distant from the melting pool) were placed closer to the weld bead where the temperatures were near to 711 °C and 622 °C, respectively. Through the TK3 and TK4 thermocouples it's shown the symmetric temperature peaks in regions close to the interface of the heat-affected Zone (HAZ) to the base metal (BM) for sample welded using pure argon as shielding gas.

Figure 2: *The welded plates with thermocouples location. a) the weld plate #WA using pure Ar as shielding gas and b) the sample #WAN with Ar+2%N_2 as shielding gas.*

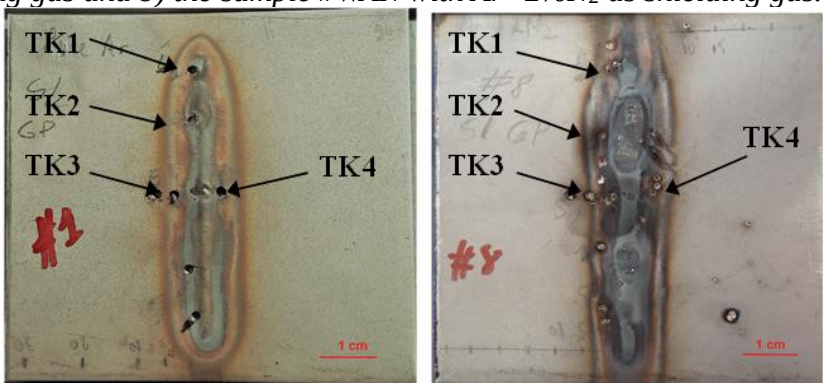

a) b)

The thermal cycle for sample Ar+2%N_2 as shown in Fig. 3 (b), a temperature peak near 736 °C is observed for thermocouple TK1 (3.0 mm distant from the melting pool) being about 25 °C higher than the obtained on pure argon sample considering the same region. Y. C. Lin *et al*. [18], also shown a peak temperature of a thermal cycle increased with increasing nitrogen content more heat is carried into shielding gas. Thus, increasing the nitrogen content is carried more heat into the workpiece and increases the weld metal area. In addition, according to the studies by K. H. Tseng and C. Chou [8], using pulsed GTAW process a greater amplitude ratio can reduce the temperature difference between the fusion zone and unaffected base metal in welding and therefore the welding residual stress can be reduced.

Figure 3: *Distribution of temperatures for samples (a) Pure Ar and (b) Ar + 2%N_2. It shows the temperature variation measured with each thermocouple for the UNS 32304 duplex stainless steel, 1.8 mm long stripe, while being welded.*

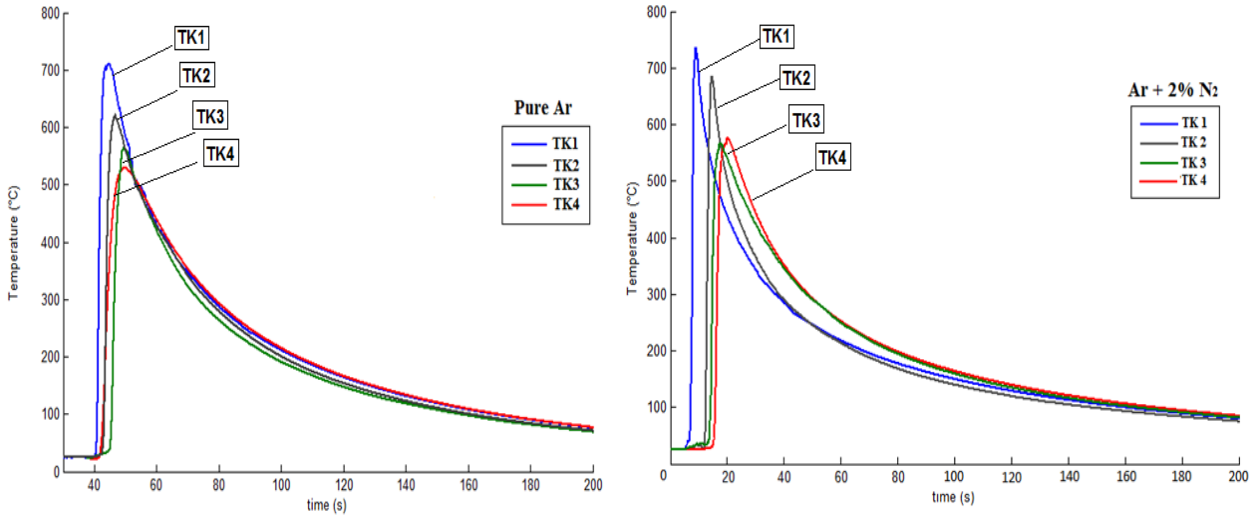

a) b)

3.2 Residual stress

Fig. 4 shows the plot strain ε x $\sin^2\psi$ for the material as received. According to $\sin^2\psi$ method, the strain vector ε is obtained through the relationship of distance between crystallographic planes calculated from diffraction pattern. So, it's observed that the slopes of the data are decreasing, indicating that the residual stresses have a compressive behavior, with values -263 ± 15 MPa for the austenite phase, and around of -192 ± 17 MPa for the ferrite phase.

As seen in Figure 5, a stress profile was found for the different phases of the samples. It is observed that in the sample welded only with pure argon, the solidified zone presented lower residual tensile strength, compared to the sample welded with shielding gas composed by the mixture argon and nitrogen. For both samples, there is a decrease in the stress state value from the heat-affected zone until base metal with original compressive residual stresses. It is also observed that the sample welded with the argon plus 2 % nitrogen protective gas flux has compressive stresses values starting at 8 mm from the center of the solidified zone, whereas the sample welded with pure argon protective flux only from 10 mm (Fig. 5(a)). This is can be correlated to the peak temperature using Ar + 2% N_2 as shielding gas observed in Fig. 4(b). A two-phase material, like DSS, is inhomogeneous,

and each phase in the material will have a different response to an applied welding heat input. As reported by Johansson *et al.* [17], the typical coefficients of thermal expansion at 100°C for both ferrite and austenite phases are 10.4 x 10^{-6} °C^{-1} and 17.2 x 10^{-6} °C^{-1}, respectively. Thus, since the two phases may have different coefficients of thermal expansion, different thermal stresses are introduced for each phase during cooling from an elevated temperature of welding.

Figure 4: *The graph ε x sin²ψ for the material as received.*

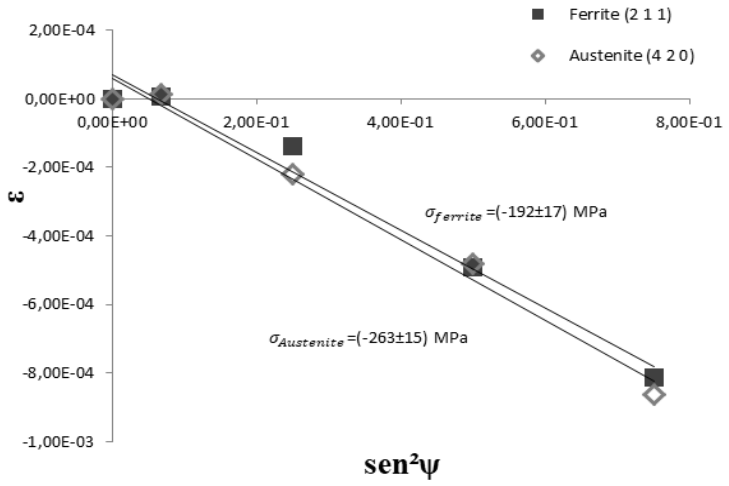

On the regions close to the heat source, the results of residual stresses obtained for the austenite, show an increase of the stress in relation to the value found for the sample as received. This may be

Figure 5: *Residual stress profiles of the austenite (a) and ferrite phases (b) of the duplex stainless steel UNS S32304 welds. The dashed line represents average residual stress (– 265 ± 13 MPa) for the as-received material.*

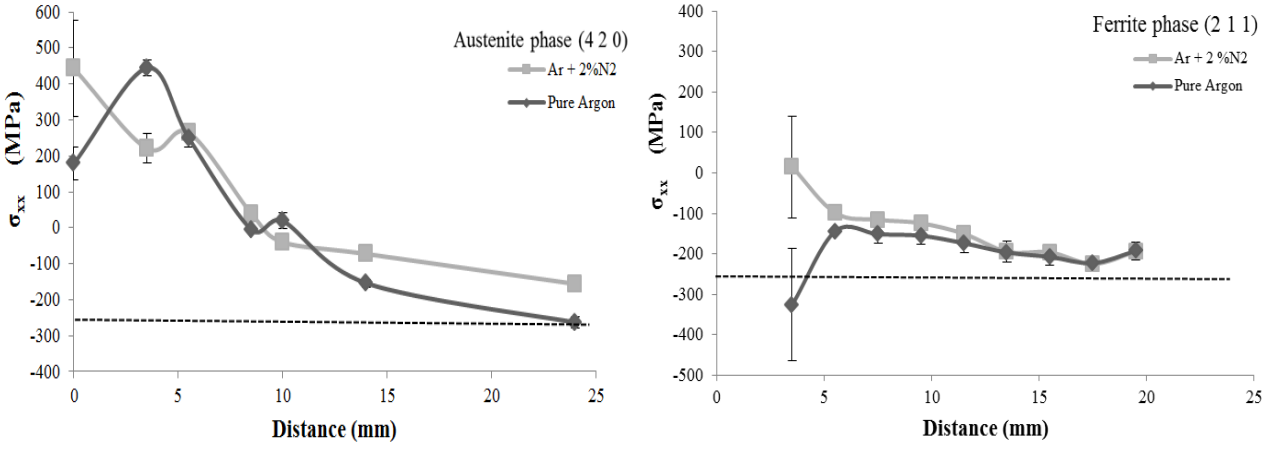

a) b)

related to the recrystallization/grain growth of the phase in this region [17].

According to Fig.5, the addition of nitrogen leads to a slight increase in the tensile residual stress of the phases. In the study made by Muthupandi *et al*. [19], the Ar-N_2 mixture has a higher ionization potential, increasing the welding energy and peak temperature. Lundin *et al*. [20] describe that additions of diatomic gases cause contraction in the contours of the plasma close to the anode. In addition they mention that the content of nitrogen increases the heat transferred by the arc into the workpiece. This can lead to distortion of plate during welding process and increased residual stress. For Hsieh *et al*. [21], it was observed that with the addition of nitrogen, the peak temperature increases and consequently the residual stresses of the austenitic steels too.

4. CONCLUSION

Based on the experimental results on a UNS S32304 duplex stainless steel, the following:

The measurement of residual stresses in samples measured by X-ray diffraction using the $\sin^2 \psi$ method, indicated that the effect of the welding thermal cycle on the heterogeneous microstructure causes the development of tensile residual stress in the solidified zone and otherwise (compressive) residual stress around 8-12 mm range away from the weld joint for both samples.

Comparison on the results for both samples revealed that the stress state is more affected by mixture using Ar+2%N_2 as shielding gas. For this kind of shielding gas, all temperature peaks are slightly higher than the ones observed in the samples using pure argon as shielding gas.

Finally, it is suggested an investigation on the gamma ray radiation interaction in welded samples of DSS for the application in the outer layer of casks for radiopharmaceuticals transport, as Type B packages. According to literature, the welds subjected to doses of ionizing radiation have a reduced capacity to resist corrosion and impact toughness, being especially true for welds made without an appropriated atmosphere.

5. ACKNOWLEDGMENT

The authors would like to express their gratitude to all colleagues of the Energy and Nuclear Research Institute (IPEN) and Federal University of Espírito Santo (UFES) responsible of the Welding Laboratory (LabSolda) for the cooperation during welding preparation. Special thanks to CAPES and CNPq for financial supports.

REFERENCES

1. HARA, D. H. S.; FIORE, M.; LUCCHESI, R. F.; MANCINI, V. A.; ROSSI, J. L. Materials selection for a transport packaging of Mo-99, In: **INTERNATIONAL NUCLEAR ATLANTIC CONFERENCE**, 2015, São Paulo. Annals of INAC 2015, São Paulo: Comissão Nacional de Energia Nuclear, 2015. p. 7.
2. CIONE, F. C.; RIZZUTTO, M. A.; SENE, F. F.; SOUZA, A. C.; BETINI, E. G.; ROSSI, J. L. The shielding against radiation produced by powder metallurgy with tungsten copper alloy applied on transport equipment for radio-pharmaceutical products, **INTERNATIONAL NUCLEAR ATLANTIC CONFERENCE**, 2015, São Paulo. Annals of INAC 2015, São Paulo: Comissão Nacional de Energia Nuclear, 2015. p. 9.
3. KANNAN, T and MURUGAN. N. Effect of flux cored arc welding process parameters on duplex stainless steel clad quality, **Journal of Materials Processing Technology,** v. 176.1, p. 230-239, 2006.
4. BETINI, E. G.; CEONI, F. C.; MUCSI, C. S.; POLITANO, R.; ORLANDO, M.T.D.; ROSSI, J.L. Study of the temperature distribution on welded thin plates of duplex steel to be used for the external clad of a cask for transportation of radiopharmaceuticals products, **INTERNATIONAL NUCLEAR ATLANTIC CONFERENCE**, 2015, São Paulo. Annals of INAC 2015, São Paulo: Comissão Nacional de Energia Nuclear, 2015. p. 6.
5. Radioactive Materials Transportation. Standard CNEN NE 5.01 Resolution CNEN 013/88Aug.1988. Available in http://appasp.cnen.gov.br/seguranca/normas/pdf/Nrm501.pdf (2017). Last accessed: 02 Jun. 2017. (In Portuguese)

6. Regulations for the safe transport of radioactive material: specific safety requirements. 2012 ed. - Vienna: International Atomic Energy Agency, 2012.
7. JIANG, Y.; TAN, H.; WANG, Z.; HONG, J.; JIANG, L.; LI, J. Influence of Cr_{eq}/Ni_{eq} on pitting corrosion resistance and mechanical properties of UNS S32304 duplex stainless steel welded joints. **Corrosion Science,** v. 70, p. 252-259, 2013.
8. TSENG, K. H. AND CHOU, C. The effect of pulsed GTA welding on the residual stress of a stainless steel weldment, **Journal of Materials Processing Technology**, v.123.3, p. 346-353, 2002.
9. MACHADO, C. S. C.; MILAGRE, M. X.; ORLANDO, M. T. D.; ROSSI, J. L.; LUZ, T. S.; MACÊDO, M. C. S.; CHAGAS, J. N. Effect of protection gas in the residual stress profile of UNS S32304 stainless steel welded with TIG, In: **Blucher Proceedings - IV Workshop of Applied Crystallography to Materials Science and Engineering**. 2014, Vitória. Annals of IV Workshop of Applied Crystallography to Materials Science and Engineering, Vitória: Grupo de Física Aplicada - UFES, 2014 p.1-4. (In Portuguese).
10. CÁRCEL-CARRASCO, F. J.; PASCUAL-GUILLAMÓN, M.; PÉREZ-PUIG, M. A. Effects of X-rays radiation on AISI 304 stainless steel weldings with AISI 316L filler material: A study of resistance and pitting corrosion behavior. **Metals**, v.6.5, pp.102, 2016.
11. MONIN, V. I.; LOPES, R. T.; TURIBUS, S. N.; PAYÃO FILHO, J. C.; ASSIS, J. T. D. X-Ray diffraction technique applied to study of residual stresses after welding of duplex stainless steel plates. **Materials Research**, v. 17, p. 64-69, 2014.
12. CULLITY, B.D. **Elements of X-Ray Diffraction**. Second Ed., Addison Wesley Inc., New York - USA, 2001.
13. CIONE, F.C.; SOUZA, A. C.; MARTINEZ, L. G.; ROSSI, J. L.; BETINI, E. G.; ROLA, F.; COLOSIO, M. A. Measurements of Residual Stresses in Aluminum Wheels Using the Techniques of XRD, Strain Gages and FEA Simulation - A Comparison. **SAE International Journal Materials and Manufacturing**, v.9, pp.1-3, 2016.
14. SAE International**, Residual Stress Measurement by X-ray diffraction,** HS-784, 3rd ed., ISBN of 978-0-7680-1069-5, 2003.
15. WITHERS, P. J.; and BHADESHIA, H. K. D. H., Residual stress. Part 1 – Measurement techniques. **Materials Science and Technology.** v. 17, pp. 355- 365, 2001.

16. WOJDYR, M. Fityk: a general-purpose peak fitting program. **Journal of Applied Crystallography,** v.43, pp. 1126-1128, 2010.
17. JOHANSSON, J.; ODÉN, M.; ZENG, X. H. Evolution of the residual stress state in a duplex stainless steel during loading. **Acta Metallurgica,** v.47.9, p. 2669- 2684, 1999.
18. LIN, Y. AND CHEN, P., Effect of nitrogen content and retained ferrite on the residual stress in austenitic stainless steel weldments, **Materials Science and Engineering A**. v.307, pp. 165–171, 2001.
19. MUTHUPANDI, V.; BALA SRINIVASAN, P.; SESHADRI, S. K.; SUNDARESAN, S. Effect of nitrogen addition on formation of secondary austenite in duplex stainless steel weld metals and resultant properties. **Science and Technology of Welding and Joining.** v. 9, pp. 47-52, 2004.
20. LUNDIN, C. D.; CHOU, C. P. D.; SULLIVAN, C. J; Hot cracking resistance of austenitic stainless steel weld metals. **Welding Journal**. v.59.8, pp. 226s-232s, 1980.
21. HSIEH, C. C.; LIN, D. Y.; CHEN, M. C.; WU, W. Precipitation and strengthening behavior of massive d-ferrite in dissimilar stainless steels during massive phase transformation**. Materials Science and Engineering, A**. v.477, pp. 328–333, 2008.